Pharmaceutical Research, Vol. 22, No. 6, June 2005 (© 2005)
DOI: 10.1007/s11095-005-4589-9

Research Paper

Insulin-like Growth Factor I–Releasing Alginate-Tricalciumphosphate Composites for Bone Regeneration

Vera Luginbuehl,[1] Esther Wenk,[1] Annette Koch,[1] Bruno Gander,[1] Hans P. Merkle,[1] and Lorenz Meinel[1,2]

Received November 15, 2004; accepted February 22, 2005

Purpose. Development and characterization of an *in situ*–forming, osteoconductive, and growth factor–releasing bone implant.
Methods. Injectable *in situ*–forming scaffolds were prepared from a 2% (m/v) alginate solution, tricalciumphosphate (TCP) granules, and poly(lactide-*co*-glycolide) microspheres (MS), loaded with the osteoinductive growth factor insulin-like growth factor I (IGF-I). Scaffolds were prepared by mixing the components followed by hydrogel formation through calcium carbonate–induced physical cross-linking of the alginate at slightly acidic pH. Physical-chemical properties and cell biocompatibility using osteoblast-like cells (MG-63 and Saos-2) of these scaffolds were investigated.
Results. The addition of TCP to the alginate resulted in reduced swelling and gelation time and an increase in stiffness. Osteoblast-like cells (MG-63 and Saos-2) did not show toxic reactions and adhered circumferentially to the TCP granules surface. The addition of the IGF-I MS resulted in an up to sevenfold increased proliferation rate of MG-63 cells as compared to scaffold preparations without IGF-I MS. The alkaline phosphate (ALP) activity—a parameter for osteblastic activity—increased with increasing amounts of TCP in Saos-2 loaded composite scaffolds.
Conclusions. A prototype *in situ*–hardening composite system for conformal filling of bone defects supporting osteoblastic activity for further clinical testing in relevant fracture models was developed and characterized.

KEY WORDS: Drug delivery systems; sustained drug delivery; Insulin-like growth factor I; Bone healing; osteoinduction.

INTRODUCTION

Injectable, *in situ* gel-forming matrices as therapeutic carriers for the treatment of musculoskeletal disorders offer several advantages over solid implants: flowable material do establish conformal filling *in vivo* during tissue (re)-generation thus avoiding gaps leading to fibrous encapsulation or scar formation, offer the possibility to co-administer therapeutic agents (e.g., growth factors) or cells, and permit minimally invasive administration (1). Injectable scaffolds for bone regeneration have been fabricated using inorganic materials, e.g., calcium phosphate (2), bioactive glass (3), synthetic polymers, e.g., poly(ethylene glycol) (4), poly(propylene fumarate) (5) and natural polymers, e.g., gelatin, hyaluronic acid, fibrin, collagen, alginate and chitosan (6). Many of these inorganic fillers and polymeric systems have been developed in the past, but all of these materials bring some difficulties that leave room for significant improvement. These difficulties revolve around issues of biocompatibility, biodegradation, toxicity, *in situ* hardening to obtain conformal filling, mechanical integrity, or the possibility to deliver drugs supporting the healing processes. This study describes the combination of an alginate gel as an *in situ* hardening system, tricalciumphosphate (TCP) as an osteoconductive filler and a slow release formulation of an osteoinductive protein, insulin-like growth factor I (IGF-I), in an effort to meet the requirements for bone fillers mentioned above.

Alginates are seaweed derived, gel-forming polysaccharides composed of 1,4-linked β-D-mannuronic (M) and α-L-guluronic (G) residues with varying proportions, forming physical gels in the presence of divalent cations such as calcium (7). The time for gelation can be controlled using poorly water-soluble calcium salts such as $CaCO_3$ or $CaSO_4$ (8). Alginates have a long history as injectable cell-delivery vehicles, cell-immobilization matrices or drug delivery systems for a variety of biological agents (7). Alginates were associated with inflammatory reactions (9), which were reduced by the use of ultrapure alginate with low M and high G block content. The M and the MG blocks, but not the G blocks were shown to stimulate cytokine production (10). The G to M block ratio is also important to control gel strength, with higher G contents resulting in higher me-

[1] Institute of Pharmaceutical Sciences, Drug Formulation and Delivery Group, Swiss Federal Institute of Technology Zurich (ETH Zurich), Zurich, Switzerland.
[2] To whom correspondence should be addressed. (e-mail: lorenz.meinel@pharma.ethz.ch)

chanical strength (11). A major drawback in using gels—including alginate gels—to fill bone defects is their insufficient mechanical support and poor mechanical integrity once the system is implanted. Therefore, additives are required to adjust the system to the mechanical needs. Suitable materials for this purpose are bioceramics such as tricalcium phosphates (TCP) and hydroxyapatite (HA) creating an osteoconductive environment which facilitates cell attachment (12). The addition of bioceramics as additives to alginate gels increased the osteoconductive potential and the mechanical properties of the implant as compared to the gel alone. Furthermore, the composite can be rendered osteoinductive through the incorporation of drugs, such as growth factors. Generally, osteoinduction requires prolonged presence of growth factors at a frequency and modality appropriate to the disease. Recently, a drug delivery system based on poly (lactide-*co*-glycolide) (PLGA) microspheres (MS) has been developed for IGF-I, and was shown to provide a controlled and sustained IGF-I release for up to 13 days (13). The IGF-I MS drug delivery system demonstrated successful osteoinduction in two different experimental fracture models performed in large animals (14).

The goal of the present study was to prepare *in situ*–hardening composites, based on i) an alginate hydrogel matrix formulated with ii) β-TCP granules and iii) a drug delivery system with a sustained and controlled release of IGF-I. The composites were characterized *in vitro* including microstructure, degradation, swelling and gelation kinetics, mechanical properties, and drug release patterns (for study design see Table I). The proliferative effect of IGF-I released from the MS and the influence of increasing amounts of β-TCP granules on alkaline phosphatase (ALP) activity were analyzed using osteoblast-like cells in combination with this novel alginate-β-TCP composite.

MATERIALS AND METHODS

Reagents

IGF-I was kindly supplied by Genentech (South San Francisco, CA, USA). Beta-tricalcium phosphate (β-TCP) granules (calc-i-oss) with a size of 100 to 300 μm was gifted from Degradable Solutions AG (Schlieren, Switzerland). Pharmaceutical grade high-viscosity sodium alginate (Manugel GMB, ISP Technologies, Girvan, Scotland) was a gift from Staerkle & Nagler AG (Zurich, Switzerland). End-group uncapped poly(lactide-*co*-glycolide) (PLGA) 50:50 (Resomer RG502H) with a molecular weight of 14 kDa was from Boehringer-Ingelheim (Ingelheim, Germany). Polysorbate 20 (Tween 20) was from Hänseler (Herisau, Switzerland). Unless specified otherwise, all other substances used were of pharmaceutical or analytical grade and purchased from Fluka (Buchs, Switzerland). Cell culture reagents were from Invitrogen (Basel, Switzerland) except otherwise specified.

Composite Preparation

For the preparation of *in situ* gelling alginate-β-TCP composites, 2.5% alginate solutions in deionized water or in 0.9% NaCl with 10 mM glucose (for cell culture experiments) were prepared. Typically, 5 mg calcium carbonate (Merck, Darmstadt, Germany) was suspended per ml 2.5% alginate solution. 0.25 ml of a fresh 0.2 mM aqueous solution of D-gluconic acid lactone (GDL) (Sigma, St. Louis, MO, USA) was stirred into 1 ml of the alginate-$CaCO_3$ suspension to initiate retarded gelation of the alginate matrix. A molar ratio of 0.54 of calcium ions to alginate carboxyl groups was used. Cylindrical composites were prepared by injecting 100 μl of the above alginate-$CaCO_3$-GDL mixture into the wells of a 96-well plate. Before complete gelation, the alginate gel was supplemented with either β-TCP granules (10, 25, 50 or 75 mg), IGF-I microspheres (IGF-I MS) as delivery system for IGF-I, or combinations thereof (Table I). IGF-I MS were prepared by microencapsulating IGF-I into end-group uncapped 14 kDa poly(lactide-*co*-glycolide) 50:50 (PLGA) (Resomer RG502H, Boehringer-Ingelheim, Ingelheim, Germany) by a double-emulsion solvent evaporation technique as previously described (13). The IGF-I dose per composite (83 μg IGF-I/cm^3) was chosen in analogy to doses of microencapsulated IGF-I shown to induce bone healing of circular (8 mm diameter; total IGF-I dose was 80 μg/cm^3) and

Table I. Study Design

	Physical-chemical properties					Cell assays		
Scaffolds	ESEM	Swelling	Gelation	Degradation	Mechanical testing	MG-63 (DNA)	Saos-2 (ALP/DNA)	IGF-I release
AL[a]	+	+	+	+	+	+	+	
AL/TCP_{10}[b]		+	+	+	+		+	
AL/TCP_{25}[b]		+	+	+	+		+	
AL/TCP_{50}[b]	+	+	+	+	+	+	+	
AL/TCP_{75}[b]		+	+	+	+		+	
AL/MS_{plac}[c]				+		+		
$AL/TCP_{50}/MS_{plac}$[b,c]				+		+		
AL/IGF-I MS[d]	+					+		+
AL/TCP_{50}/IGF-I MS[b,d]	+					+		+

[a] AL: alginate matrix.
[b] AL/TCP_X: alginate matrix + X mg TCP per scaffold.
[c] AL/MS_{plac}: alginate + placebo (empty) microspheres (MS).
[d] AL/IGF-I MS: alginate + IGF-I MS.

segmental (10 mm gap; total IGF-I dose was 100 μg/cm^3) femoral defects in sheep (14).

IGF-I Loading and Release

IGF-I loading was determined as described before (15). Briefly, 50 mg of microspheres were dissolved in 0.3 ml DCM. Then, 0.7 ml of acetone were added, and the vial vortexed and centrifuged at 20,000 rcf for 5 min. The supernatant was removed, and 0.9 ml of a 3:1 acetone:DCM mixture was added (n = 3). This washing procedure was repeated three times. Finally, the residue was dissolved in 0.1 M acetic acid. IGF-I was assayed by HPLC using a Merck system (Dübendorf, Switzerland) consisting of a sample cooler, an autoinjector (A4000), a computer interface (A6000), a pump (6200A), and UV (L4250) and fluorimetric (F 1050) detectors. Separation was performed on a Zorbax 300SB CN column (150 × 4.6 mm) at 40°C, under gradient conditions at a flow rate of 0.8 ml/min. Two eluents were used, (A) consisting of 5% acetonitrile and 0.2% trifluoroacetic acid (TFA) in water and (B) 80% acetonitrile and 0.2% TFA in water. The solvent was initially composed of 74% (v/v) eluent A. The solvent was changed over 30 min to 100% eluent B. Then, initial conditions were set to wash the column. IGF-I was detected at 214 nm and quantified by measuring the peak area.

In vitro release from IGF-I loaded microspheres as a function of loading, presence of TCP granules, alginate gel, or both was determined in 1.5 ml release medium (50 mM sodiumacetate, 100 mM sodiumchloride, 0.02% Polysorbate 20, 0.02% sodiumazide, pH 5.4; release medium was chosen to preserve IGF-I structure and activity—no effect of storage at 37°C on IGF-I stability (HPLC, ELISA) or bioactivity (MG-63 cell culture) was observed for control IGF-I solutions diluted in this release medium (measured at day 0 and day 3; data not shown). The following formulations were evaluated: i) 8.3 μg IGF-I in 11.2 mg MS with 50 mg TCP granules suspended in 100 μl alginate matrix, ii) 16.6 μg IGF-I in 22.4 mg MS with 50 mg TCP granules suspended in 100 μl alginate matrix, iii) 8.3 μg IGF-I in 11.2 mg MS, no TCP, no alginate iv) 8.3 μg IGF-I in 11.2 mg MS, no TCP and suspended in 100 μl alginate matrix, and v) 8.3 μg IGF-I in 11.2 mg MS with 50 mg TCP granules, no alginate. The release medium was fully exchanged with fresh medium after 9.5, 32, 53, 72, 97 h, and 7, 10, 14, 21, and 28 days, respectively. Medium samples were immediately frozen at −20°C (freezing has no effect on stability (HPLC, ELISA), or bioactivity (MG-63 cell based proliferation assay; data not shown), and analyzed using an IGF-I enzyme-linked immunosorbent assay (ELISA; DuoSet Human) according to the manufacturer's protocol (R&D Systems, Minneapolis, MN; n = 3–4).

Environmental Scanning Electron Microscopy (ESEM)

The microstructures of the composites were characterized using an ESEM (FEI/Philips XL 40, FEI Company, Hillsboro, OR) at 10 kV. Composites were washed with deionized water to remove salt before measuring and cut longitudinally in half. Composites were analyzed without any further pretreatment by ESEM.

Swelling Kinetics

Composites were incubated in 2 ml 0.1 M Tris buffer (pH = 7.4) in 12-well plates at 37°C, and wet weights were determined at different time points. The degree of swelling (Q), was calculated according to the following formula: as elsewhere described (16):

$$Q = \left[(1/\rho_p) \left[Q_m/\rho_s + 1/\rho_p \right]^{-1} \right]^{-1}$$

where ρ_p is the polymer density (calculated for each composite, mg/mm^3), ρ_s is the density of water, and Q_m is the swelling ratio, defined as the mass ratio of absorbed water to the dried gel. To obtain Q_m, the weight of swollen composites and the weight of dried composites following drying over night at 50°C were measured.

Rheological Measurements

The rheological properties were examined using a HAAKE RheoStress 600 rheometer (Thermo Electron GmbH, Karlsruhe, Germany) with a plate–plate measuring geometry with a diameter of 35 mm and a plate to plate distance of 1 mm. To avoid water evaporation during measurements a solvent trap system served to create a humified atmosphere around the probe.

Gelling kinetics as a function of the amount of supplemented β-TCP granules (0, 10, 25, 50 and 75 mg/composite) added to the alginate gel were characterized by determination of storage (G′) and loss (G″) moduli from the oscillating measurements with a controlled deformation of 0.05% at a frequency of 1 Hz. Gelation was initiated by adding GDL, then 1 ml probe was placed on the rheometer plate preheated to 37°C. Gelation time was estimated at the intersection of G' and G'' (17).

Composite Degradation

Degradation of different composite preparations was evaluated by monitoring the changes in weight loss over time. Composites (n = 6) were incubated in minimum essential medium (MEM) containing 10% FBS, supplemented with penicillin (100 units/mL)/streptomycin (100 μg/mL) and 0.01% sodium azide at 37°C.

Mechanical Testing

To evaluate the influence of different amounts of β-TCP granules on the mechanical properties of the gels, formulations with 0, 10, 25, 50, or 75 mg of β-TCP granules per 100 μl alginate were molded into the wells of a 96-well plate and allowed to cure over night before testing. Three sample composites of each formulation were tested. Uniaxial compression was performed on a mechanical tester (Instron 1122; Instron Corp., Canton, MA, USA), equipped with a 50 N loading cell at a deformation rate of 1 mm/min. An initial load of 0.01 N was applied. Young's Modulus was calculated from the slope of the strain-stress curve within the linear region up to 10% strain.

Cells, Cell-Seeding, and Culture of Three-Dimensional Composites

Two human osteoblast-like cell lines MG-63 and Saos-2 (ATCC, Manassas, VA, USA) were used in these experiments. MG-63 cells were cultured in minimum essential medium (MEM) containing 10% heat inactivated FBS, supplemented with a mix of penicillin (100 units/ml), streptomycin (100 μg/ml), amphotericin B (5 μg/ml), L-glutamine (2 mM), sodium pyruvate (1 mM), and nonessential amino acids (0.1 mM) at 37°C in a humidified atmosphere containing 5% CO_2. Saos-2 cells were cultured in DMEM (Dulbecco's modified Eagle medium) with L-glutamine (2 mM), D-glucose (4500 mg/ml), and sodium pyruvate (1 mM) containing 10% heat inactivated FBS, supplemented with a mix of penicillin (100 units/ml), streptomycin (100 μg/ml), amphotericin B (5 μg/ml) and nonessential amino acids (0.1 mM). Cells were harvested at 90% confluence, counted, and immediately used to seed the composites.

Before complete gelation of the composites, 2×10^4 MG-63 or Saos-2 cells were injected into the cylinders ($n = 6$) and thoroughly mixed into the scaffold matrix. Composites were allowed to harden at 37°C in a humidified atmosphere containing 5% CO_2 for 2 h. After removal from the 96-well plate, they were transferred to 24-well plates and cultured in 1 ml cell culture medium for 2 and 7 days under mild agitation (160 min^{-1}) on a horizontal shaker. Medium was exchanged after 2 h to avoid calcium deprivation of the culture medium and, thereby, impact the cells's performance. Medium was thereafter exchanged every other day. Alginate gels without cells were cultured in the same way and used as controls.

DNA Quantification

DNA quantification was performed to assess cell proliferation in the different composite formulations. After incubation of cell-seeded and unseeded (control) composites for 2 to 7 days, composites were rinsed three times with PBS and lysed in 0.2% Triton X-100, 10 mM Tris (pH = 7.4) containing 54 mM EDTA for 2 days. Supernatants were used to quantify total DNA content in the composites using a fluorescence assay (PicoGreen dsDNA Quantitation Kit, Molecular Probes, Leiden, Netherlands) according to the instruction of the manufacturer.

Alkaline Phosphatase Activity

Saos-2-cell seeded and composites without cells were cultured for 2 and 7 days, rinsed three times with PBS and lysed in 0.2% Triton X-100 (Fluka, Buchs, Switzerland), 10 mM Tris (pH = 7.4) containing 54 mM EDTA at 4°C. Supernatants of lysed composites were used to measure ALP activity as described before (18). For this, 100 μl aliquots of the lysates were added to 100 μl working reagent in a 96 well culture plate for 30 min at 37°C. The working reagent consisted of a 1:1:1 (v/v/v) mixture of 0.5 M 2-amino-2-methylpropanol (pH = 10.5) (Sigma, Steinheim, Germany), 5 mM p-nitrophenolphosphate, and 5 mM magnesium chloride. After development of colour, the time was recorded and the reaction stopped by adding 100 μl of 0.3 M sodium hydroxide, and the final absorbance was read at 405 nm using a microplate reader (ThermoMax, Molecular Devices, Sunnyvale, CA). ALP activity was expressed as nanomoles p-nitrophenol per ng DNA and normalized to the time needed for the reaction in minutes.

Confocal Fluorescence Microscopy (CLSM)

To assess MG-63 cell viability and morphology in the composites, an *in situ* fluorescence viability study was performed with a Live–Dead viability/cytotoxicity kit (Molecular Probes). Cell seeded composites (MG-63 cells) cultured for 2 and 7 days were washed three times with PBS, and then incubated in 5 μM Calcein AM, 5 μM ethidium homodimer-1 and 10 μM Hoechst 33342 (Molecular Probes) for 30 min in PBS. Composites were cut longitudinally in half and incorporated cells were observed immediately. Brightfield and fluorescence images were obtained with a Zeiss 410 inverted microscope with Plan-Neofluar 10×, 20×, and 40× objectives (Zeiss, Jena, Germany), equipped with Argon (488 nm) and HeNe (543 nm) lasers for fluorescence. Background fluorescence was determined by analyzing composites without cell seeding. Two-dimensional multi-channel image processing was performed using IMARIS (Bitplane AG, Switzerland).

Statistics

Statistical analysis of data was performed by one-way analysis of variance (ANOVA) and Tukey–Kramer procedure for *post hoc* comparison using Minitab (Minitab Inc., State College, PA, USA). p values less than 0.05 were considered statistically significant. Areas under the Curve (AUC) were determined using Sigma Plot (Systat, Point Richmond, CA).

RESULTS

Composite Characteristics

The alginate gel surface was generally flat, nonporous and covered with protuberances as determined by ESEM (Fig. 1A). The addition of β-TCP granules into the alginate matrix resulted in a porous microstructure with granule sizes ranging from 100 to 300 μm (Fig. 1B). IGF-I loaded MS with a mean diameter of about 50 μm mixed to the alginate gel (Fig. 1C) also increased the gel porosity. Addition of IGF-I MS together with β-TCP granules resulted in a homogenous distribution of both particle types and the gel matrix was more porous than that of the pure alginate gel (Fig. 1D). The swelling curves of all formulations were characterized by a rapid increase of the swelling ratio Q within the first hour of incubation, followed by a slight shrinkage of the gel matrix resulting in a plateau after about 4 h (Fig. 2). The total amount of composite swelling was inversely dependent on the amount of β-TCP granules added. The alginate matrix without β-granules had a swelling ratio of 31.0 ± 1.8, whereas the addition of β-TCP granules resulted in a decrease of the swelling ratio from 11.6 ± 0.9 to 4.1 ± 0.7 of 10% and 75% (all w/w) addition of TCP granules to the gel, respectively.

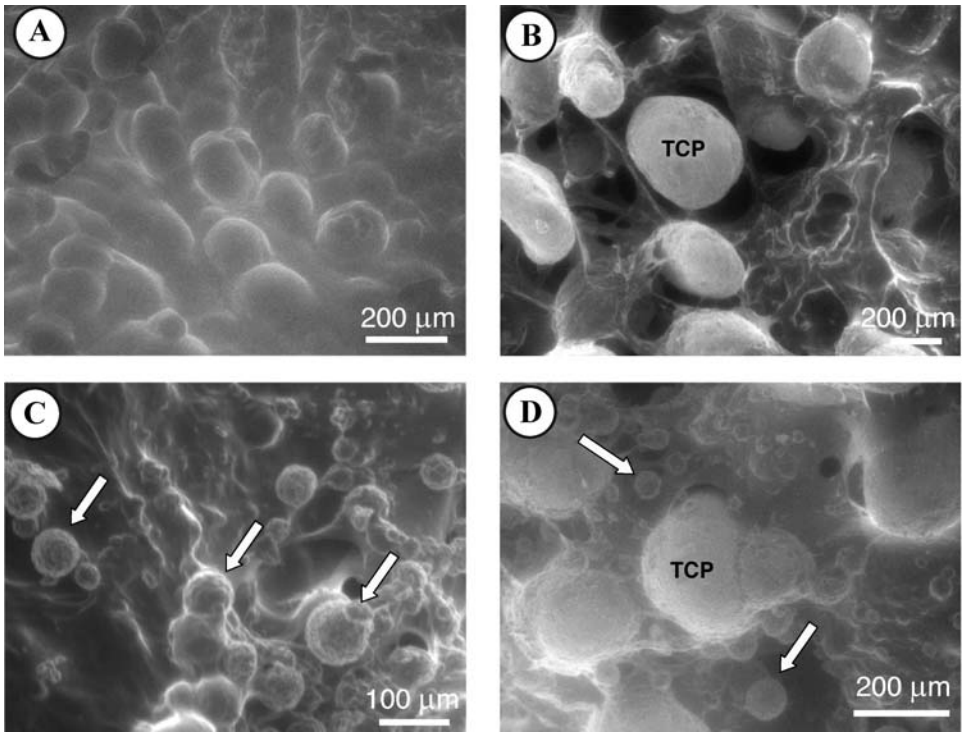

Fig. 1. Environmental scanning electron microscopy (ESEM) of surface morphology. (A) alginate matrix, (B) alginate with β-TCP granules (AL/TCP_{50}), (C) alginate with IGF-I microspheres (AL/IGF-MS), (D) alginate matrix with β-TCP granules and IGF-I MS (AL/TCP_{50}/IGF-MS). IGF-I MS are highlighted by arrows.

For the preparation of the composites, GDL was used to initiate retarded gelation. The lactone hydrolyses slowly and, thereby, gradually lowers the pH resulting in a slow release of calcium ions from $CaCO_3$, which becomes soluble at lower pH (19). Gelation time was found to depend on the amounts of β-TCP granules added to the gel matrix (Fig. 3). An inverse relation between gelation time and β-TCP granule amount was found. The alginate gel without β-TCP granules gelated within 35 minutes as compared to 15 minutes for the composites with 75% β-TCP granules.

Simulated body fluid was used to study degradation kinetics of alginate and alginate composites (Table II). After 27 days of incubation, alginate gels had a weight loss of 55% and composites a weight loss between 33 and 39%. The presence of placebo microspheres did not effect the degradation (Table II).

The mechanical properties of the composites were measured in compression tests and with increasing amounts

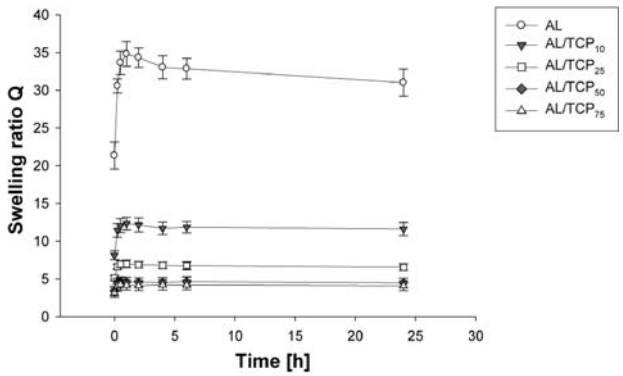

Fig. 2. Swelling behavior over 24 h of alginate gel matrix (AL) and composite scaffolds (AL/TCP_X) with different amounts (X) of TCP granules embedded in the gel matrix as indicated by the numbers.

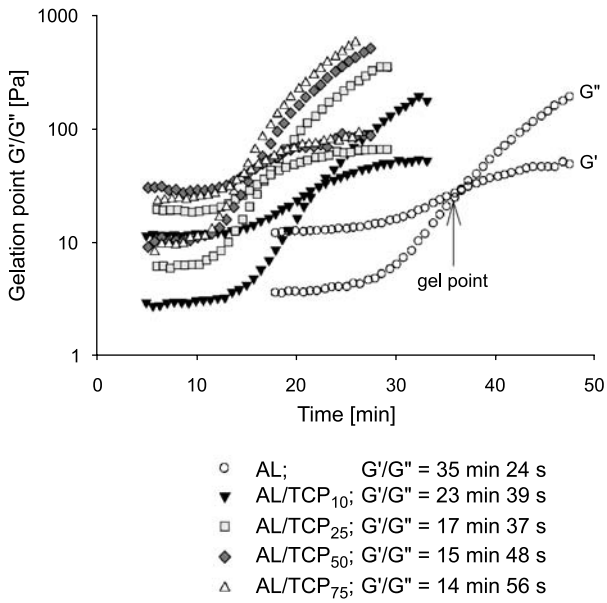

Fig. 3. Oscillatory rheological measurements were used to analyze the gelling kinetics of the matrices depending on the amounts of β-TCP granules (0, 10, 25, 50 and 75 mg/scaffold) added to the alginate gel. The gel point was estimated by the crossover of storage (G′) and loss (G″) modulus highlighted at the curve of the alginate gel by an arrow.

Table II. *In Vitro* Degradation Kinetics of Alginate Scaffolds with Different Amounts of TCP (10, 25, 50, 75 mg) with or without Placebo Microspheres (MS_{plac})

Scaffolds	Weight (%)					
	1 day	2 days	7 days	14 days	21 days	27 days
AL/TCP_{10}[b]	93.8 ± 2.7	84.1 ± 2.6	77.6 ± 2.2	68.6 ± 2.0	62.7 ± 4.5	61.0 ± 3.1
AL/TCP_{25}[b]	96.0 ± 5.6	88.1 ± 6.2	79.9 ± 6.1	73.6 ± 6.2	68.9 ± 8.6	67.0 ± 8.1
AL/TCP_{50}[b]	65.1 ± 9.4	69.7 ± 9.1	65.2 ± 9.5	67.0 ± 10.2	65.2 ± 9.4	61.7 ± 4.5
AL/TCP_{75}[b]	87.3 ± 3.5	89.9 ± 8.3	84.7 ± 10.6	82.6 ± 13.2	79.5[d]	[e]
AL[a]	89.6 ± 7.1	83.6 ± 7.6	73.8 ± 6.6	66.3 ± 7.2	60.9 ± 6.9	45.4 ± 12.8
AL/MS_{plac}[c]	68.9 ± 17.0	62.0 ± 11.5	61.7 ± 6.8	73.3 ± 8.2	75.5 ± 8.2	60.0 ± 8.7
$AL/TCP_{50}/MS_{plac}$[b,c]	69.1 ± 18.8	73.1 ± 19.1	71.1 ± 19.2	77.3 ± 21.4	73.4 ± 19.4	67.3 ± 17.7

[a] AL: alginate matrix.
[b] AL/TCP_X: alginate matrix + X mg TCP per scaffold.
[c] AL/MS_{plac}: alginate + placebo (empty) microspheres (MS).
[d] No standard deviation due to scaffold degradation.
[e] Degraded.

of β-TCP granules in the alginate matrix, Young's modulus (YM) increased in a non linear way (Fig. 4). A 15-fold increase in this modulus was observed for the composite with 75% β-TCP granules (176.8 ± 35.6 kPa) as compared to the alginate gel without β-TCP granules (11.8 ± 0.6 kPa).

IGF-I Loading and Release

The total loading was 0.738 ± 0.139 μg IGF-I per mg PLGA MS as determined by HPLC. For evaluation of *in vitro* IGF-I release, 11.2 mg of IGF-I loaded PLGA MS, corresponding to a total dose of 8.3 μg IGF-I, was incorporated into 100 μl of alginate matrix, with or without addition of 50 mg β-TCP granules. Additionally, similar composites were prepared with 22.4 mg microspheres, corresponding to 16.6 μg IGF-I, to evaluate the effect of total IGF-I dose on release patterns (Fig. 5A and B). Generally, the release curves were similar for the high loading (total IGF-I dose 16.6 μg) and the lower loading (total IGF-I dose 8.3 μg). However, the initial burst was significantly higher for the higher IGF-I loading after 9.5 h ($p < 0.05$) and significantly higher for the lower loading after 32 h ($p < 0.05$). This initial release was followed by a lag phase lasting up to 7 days and characterized by a minimal release of IGF-I. From day 7 on, a steep increase in IGF-I release was simultaneously observed for both formulations, with the higher loaded formulation releasing significantly more IGF-I than the lower loaded formulations at all time-points ($p < 0.01$ or $p < 0.05$). A difference between the groups after 28 days when compared to the 21 days time-point was observed, with a declining release rate for the formulation with the higher loading ($p < 0.05$), while the release from the formulation with the lower loading, although not statistically significant, continued to rise (Fig. 5A). This finding, along with an apparent increase in standard deviations observed for all formulations after 28 days as compared to previous time-points, suggest the beginning decline of IGF-I release from the formulations (Fig. 5A–C). The total amount of released IGF-I (AUC) was more than two times higher for the higher loaded formulation (total IGF-I dose 16.6 μg) as compared to the formulation with the lower loading (total IGF-I dose 8.3 μg; $p < 0.01$; Fig. 5B).

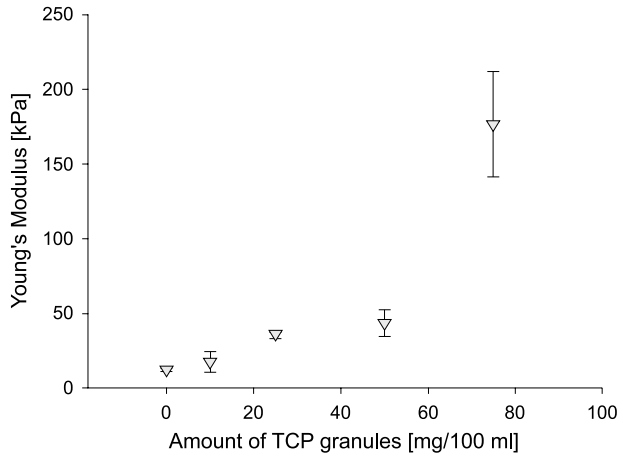

Fig. 4. Young's Modulus (YM) of composite scaffolds with different amounts of β-TCP granules (0, 10, 25, 50, 75 mg/scaffold).

Furthermore, the impact of the alginate matrix, or the TCP granules, or both on release kinetics and the resulting areas under the curve were assessed (Fig. 5C and D). Generally, the release curves were similar for all groups, characterized by an initial burst (days 1 and 2), a lag phase with minimum release (days 2 to 7) and a steep increase in IGF-I release form day 7 on. The curve progression was reproducible, besides from the initial burst and after 28 days, when the standard deviations were larger as compared to the other time-points. The presence of TCP minimally influenced the release as compared to the IGF-MS alone ($p < 0.05$). However, the presence of the alginate matrix, with or without addition of TCP granules, resulted in a decrease of the AUC as compared to the IGF-MS alone or the mixture of IGF-I with TCP granules ($p < 0.01$; Fig. 5C and D).

Cell Viability, Proliferation and ALP Activity

Cellular viability, proliferation, IGF-release kinetics and activity within the composites were tested with two different osteoblast-like cell lines (MG-63 and Saos-2; for study design

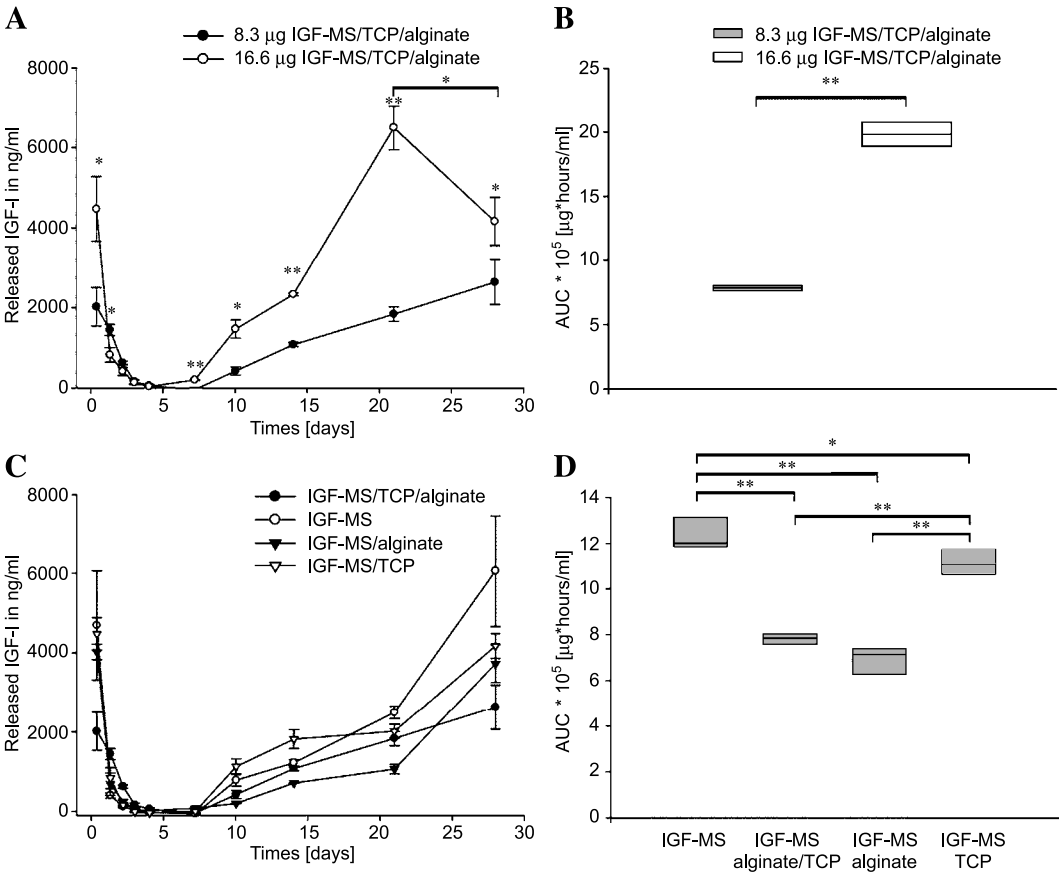

Fig. 5. IGF-I release over 28 days as determined by ELISA. (A) IGF-I release and (B) IGF-I area under the curve (AUC) from alginate matrix formulations loaded with TCP granules and a total IGF-I dose, encapsulated in PLGA MS, of 8.3 µg or 16.6 µg, respectively. (C) IGF-I release kinetics and (D) IGF-I area under the curve from formulations containing 8.3 µg IGF-I, encapsulated in PLGA-MS. The formulations were composed of IGF-I PLGA MS with TCP granules in alginate matrix (IGF-MS/TCP/alginate), IGF-I MS only (IGF-MS), IGF-I MS in alginate matrix (IGF-MS/alginate), and IGF-I MS with TCP granules (IGF-MS/TCP). (**$p < 0.01$, *$p < 0.05$).

see Table I) (20,21). The cells were carefully mixed with the alginate formulation during gel formation avoiding high shear forces. Cylindrical alginate gels (dimensions of 5 × 4 mm), loaded with IGF-I PLGA MS and MG-63 cells, were prepared with or without TCP granules. These constructs were incubated in cell culture medium for 7 days at 37°C (Fig. 6). The IGF-I concentrations in the supernatant of MG-63 cell seeded gels was characterized by an initial burst of about 12% of the total loading. This phase was followed by a phase of minimal IGF-I release as measured by ELISA. After 7 days about 18% of the total encapsulated IGF-I was released and no differences between the groups—TCP loaded or unloaded—were observed (Fig. 6).

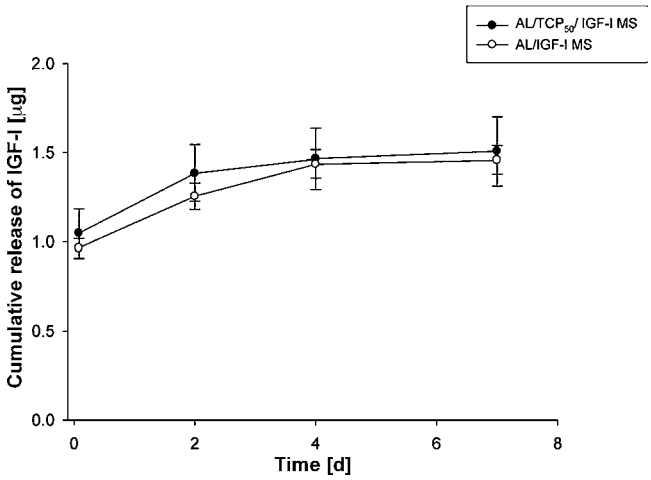

Fig. 6. Cumulative IGF-I release from PLGA MS embedded in alginate gel matrix with or without β-TCP granules as measured in the supernatant of the cell culture studies (MG-63 cells).

The MG-63 cells, a cell line frequently used to assess IGF-I bioactivity (22,23), were selected to examine cellular proliferation based on total DNA quantification (24). No significant differences in proliferation rates were observed after 2 days, except for the formulation with β-TCP granules/placebo MS, where DNA concentration was reduced to 50% of the DNA initially present in the cell seeded composite ($p < 0.05$) (Fig. 7A). After 7 days, all formulations without IGF-I MS dropped to significantly lower DNA contents as compared to the alginate gel matrix ($p < 0.01$). CLSM images showed that MG-63 cells were localized in cell clusters within the alginate gel with no apparent adherence to the gel matrix (Fig. 7B, panel a). In contrast, the presence of β-TCP granules resulted in circumferential adherence of the cells to the rough and porous β-TCP granule surface (Fig. 7B, panel b). Very few dead cells were observed, except for placebo MS

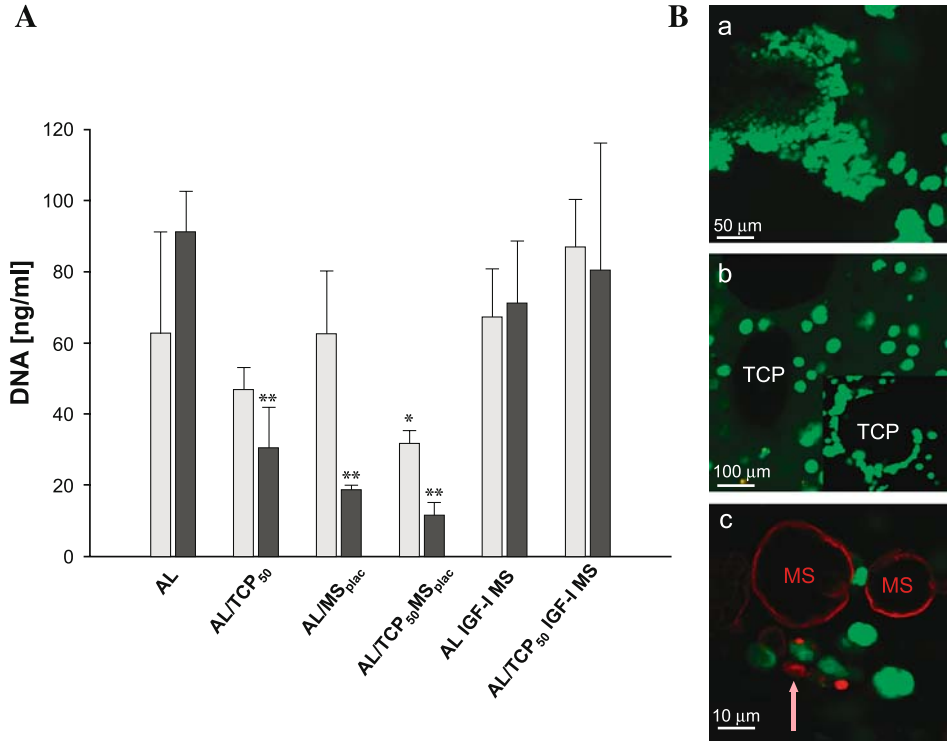

Fig. 7. (A) DNA content analyzed from different scaffold formulations (AL: alginate, TCP: β-TCP granules, MS: microspheres) seeded with osteoblast-like cells (MG-63) cultured for 2 (light gray bars) and 7 (dark gray bars) days. (**$p < 0.01$, *$p < 0.05$). (B) CLSM images after 7 days of culture of MG-63 cells seeded on (a) alginate, (b) composites with 50 mg TCP granules, or with (c) placebo microspheres (MS). Cells were stained with calcein and ethidium homodimer to distinguish living (green fluorescent) and dead cells (red fluorescent); see arrow in (c).

formulation, where a few dead cells were observed particularly close to placebo MS (Fig. 7B, panel c). The total cell number appeared to drop in regions more than 500 µm below the surface, as assessed qualitatively by CLSM.

A marker of osteogenic activity, alkaline phosphatase (ALP) activity, was analyzed as a function of composite formulations using the osteoblastic Saos-2 cell line (for study design see Table I). An increase in ALP activity is characteristic for the mineralizing osteoblast (25). Because the MG-63 cells express very little ALP (26), Saos-2 cells were used to examine ALP activity as a function of the different formulations (27). The influence of increasing amounts of β-TCP granules (0, 10, 25, 50, 75 mg/composite) on ALP activity was also determined (Fig. 8). In all formulations ALP activity normalized to DNA content was significantly higher at day 7 as compared to day 2 ($p < 0.05$) (Fig. 8A). ALP activity was more than 3 times higher in composites containing β-TCP granules (Fig. 8A) as compared to the alginate matrix prepared without β-TCP granules at days 2 and 7, respectively ($p < 0.01$). ALP activity increased from 29.6 ± 9.5 to 108.3 ± 77.8 (nM pNP min^{-1} ng^{-1} DNA) after 2 days, and from 47.2 ± 15.7 to 435.3 ± 137.4 (nM pNP min^{-1} ng^{-1} DNA) after 7 days with increasing amounts of β-TCP granules (10, 25, 50, 75 mg per composite), respectively. The amount of DNA, unlike in MG-63 cells (Fig. 5A), decreased from day 2 to 7, with significantly lower DNA contents for preparations with increasing proportions of β-TCP granules ($p < 0.05$ or 0.01) (Fig. 8B).

DISCUSSION

Injectable *in situ*–hardening composites were developed consisting of an alginate hydrogel matrix with incorporated β-TCP granules and PLGA-MS for sustained IGF-I release as an option for minimally invasive osteoconductive and osteoinductive treatments of bone defects. Physicochemical properties and cellular biocompatibility of these composite scaffolds were tested (for study design see Table I). The composite formulations showed reduced swelling, faster gelation and improved compressive stiffness with increasing amounts of incorporated β-TCP granules as compared to alginate gel alone. All scaffolds were stable in a simulated body fluid for up to 4 weeks. The IGF-I release and the total amount of released IGF-I were determined with and without TCP granules or alginate matrix over 28 days. Osteoblast-like cells (MG-63 and Saos-2) seeded on the scaffolds showed good cell viability after 2 and 7 days in particular in the outer scaffold regions with cells predominantly adhering to the surface of TCP granules. The release of bioactive IGF-I from MS incorporated in the scaffolds significantly enhanced the proliferation rates of MG-63 cells.

The successful use of bone defect fillers requires detailed knowledge and control of swelling, gelation time, degradation and mechanical properties of the implant. The addition of β-TCP granules to the alginate hydrogel resulted in more rigid material characteristics (Fig. 1B) as compared to the alginate gel alone (Fig. 1A) and, therefore, in decreased

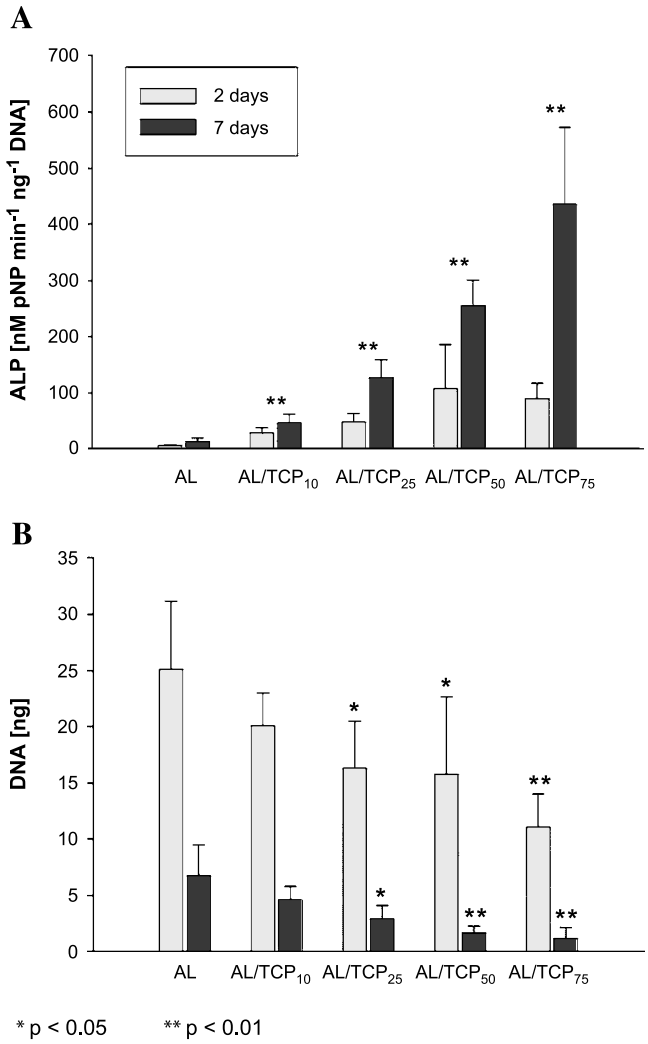

Fig. 8. (A) Alkaline phosphatase (ALP) activity and (B) DNA content of Saos-2 cells seeded in matrices containing different amounts of β-TCP granules (0, 10, 25, 50, 75 mg/scaffold). (**$p < 0.01$, *$p < 0.05$).

swelling ratios (Fig. 2) and increased mechanical stability (Fig. 4). However, in comparison to the compressive modulus of human trabecular bone (50 MPa) (28), the compressive modulus of the developed composites (up to 200 kPa) clearly demonstrated that the alginate β-TCP composites should find application in load-bearing bones together with external stabilization, e.g., by the use of a fixateur externe or plates.

The gelation time of the scaffolds shortened with increasing amounts of β-TCP granules (Fig. 3). Faster gelation could be a result of the higher initial viscosity due to incorporated β-TCP granules as seen in the higher initial values of the storage modulus G′ (Fig. 3). Furthermore, calcium release from the surface of TCP granules may lead to increased gelation times, especially at low pH as a result of the addition of the GDL. However, generally only minimal amounts of extra calcium are released from β-TCP, even at slightly acidic pH and, therefore, most likely this effect had an insignificant impact on the formation of the composites. For example, calcium release from β-TCP during *in vitro* degradation at pH 5.6 was described to be in the range of 54 ppm after 1 h (29).

The *in vitro* degradation of our formulations (mass loss of 33 to 55% after 4 weeks; Table II) was in the range of *in vivo* degradation rates reported for alginate formulations, which were implanted subcutaneously into the back of mice and had a mass loss of almost 55% after 6 weeks (30).

The *in vitro* release pattern was evaluated at pH 5.4 over 28 days. This non-physiological release medium was chosen to preserve IGF-I structure and activity overtime, as we have shown before (VL unpublished data). The presence of alginate significantly reduced the total amount of released IGF-I (Fig. 5D), a finding which has been previously reported for other proteins including bovine serum albumin (BSA) (31), basic fibroblast growth factor (bFGF) (32), and vascular endothelial growth factor (VEGF) (31,33–36). IGF-I has a pI of 8.4 (37,38), whereas the pKa value for alginate is about 3.5 (39). At pH 5.4 (Fig. 5) or 7.4 (Fig. 7) IGF-I carries a positive net charge and, therefore, can interact electrostatically with alginate, which is negatively charged. Similar findings were reported for VEGF (pI 8.5) (31), whereas BSA (pI 4.7), has much lower electrostatic interactions (31,40). For further development of the IGF-I formulations BSA might, therefore, be added as an excipient to mask the electrostatic IGF-alginate matrix interaction, in an effort to strictly confine the control of drug delivery to the degrading PLGA-MS while minimizing the impact of the alginate matrix.

The development of this formulation towards clinical use needs further studies detailing the osteoinductive responses kick-started upon implantation into defect sites. Besides from the important information revolving around *in vivo* performance, further questions can be addressed, revolving around optimized kinetics. More specifically, the release kinetics presented here, as determined at pH 5.4 (Fig. 5) and corroborated for time points earlier than 7 days at pH 7.4 (Fig. 6), coincide with the chondrogenic (days approx. 7–25 post-trauma) and osteogenic (days approx. 12–30 post-trauma) phases in physiological, endochondral bone healing, as detailed for segmental and circular defects in mice, rats (41–43), and sheep (L.M., unpublished results). During these physiologic healing events, both the chondrogenic and osteogenic phases are characterized by high expression levels of IGF-I (LM, unpublished results) (42). Based on the hypothesis that the defect zone is most susceptible to an IGF-I triggered osteoinductive stimulus when release kinetics match the endogenous production of IGF-I, the biomimetic release profiles as presented here might induce more potent osteoinductive stimuli than other release profiles. Apparently, further studies are needed to detail the hypothesized advantage of biomimetic over other release profiles and the presented systems offers a good platform to start-off working in that direction.

ALP activity of Saos-2 cells seeded into alginate gels alone was low (Fig. 8A), and significantly increased with increasing amounts of β-TCP granules added to the gel matrix. These findings demonstrate that β-TCP granules supported the osteoblastic activity of Saos-2 cells. The two cell lines selected in this study (Saos-2 cells and MG-63 cells) are often commonly referred to as (pre)osteblastic cell lines. Although a common expression is used for both cell lines, it should not belie the fact that striking differences do exist

between them, also reflected by the results reported here, e.g., by the markedly different proliferation of MG-63 cells vs. Saos-2 cells, although cultured at identical conditions (Figs. 7A and 8B). Saos-2 cells, unlike MG-63 cells, exhibit many features of a well-differentiated osteoblast including the ability to induce mineralization of their matrix (20,21,44). It has been described for several progenitor cells that a progression towards the ultimate phenotype can be correlated with a decrease in proliferation rates, including osteoblast progenitors (45). The MG-63 cell line more closely resembles osteoblastic progenitors in less differentiated stages, whereas the Saos-2 cell line exhibits more advanced differentiation. The more advanced stage of Saos-2 cells is also reflected by the reported results, as these cells showed reduced proliferation with increasing amounts of β-TCP granules (Fig. 8B), a result similarly reported for primary osteoblasts derived from rat calvarial cells (46).

The presented injectable composite system consisting of an alginate gel, TCP granules, and PLGA-MS for the sustained release of the osteoinductive growth factor IGF-I has interesting features for orthopaedic applications, combining the option for conformal filling of the defect, increased mechanical stability, an osteoconductive environment (TCP granules and microspheres) with an osteoinductive stimulus (controlled release of growth factors). This renders this pharmaceutical system an interesting tool for the treatment of bone defects and for future animal studies using fracture models.

ACKNOWLEDGMENTS

We thank Sandra Hubl for technical assistance and Romain Voide and Matthias Goessi for support revolving around the mechanical testing experiments. Further thanks go to Dr. P. Ott for taking the ESEM images, Dr. Kurt Ruffieux and Dr. Fabrice Maspero for supply with TCP granules, and Sandra Hofmann for support with the statistical analysis. IGF-I was kindly provided by Genentech, South San Francisco, CA, USA (Dr. Jeff Cleland).

REFERENCES

1. A. S. Hoffman. Hydrogels for biomedical applications. *Adv. Drug Deliv. Rev.* **54**:3–12 (2002).
2. B. R. Constantz, I. C. Ison, M. T. Fulmer, R. D. Poser, S. T. Smith, M. VanWagoner, J. Ross, S. A. Goldstein, J. B. Jupiter, and D. I. Rosenthal. Skeletal repair by *in situ* formation of the mineral phase of bone. *Science* **267**:1796–1799 (1995).
3. L. L. Hench, I. D. Xynos, and J. M. Polak. Bioactive glasses for *in situ* tissue regeneration. *J. Biomater. Sci. Polym. Ed.* **15**:543–562 (2004).
4. J. A. Burdick, M. N. Mason, A. D. Hinman, K. Thorne, and K. S. Anseth. Delivery of osteoinductive growth factors from degradable PEG hydrogels influences osteoblast differentiation and mineralization. *J. Control. Release* **83**:53–63 (2002).
5. R. G. Payne, M. J. Yaszemski, A. W. Yasko, and A. G. Mikos. Development of an injectable, *in situ* crosslinkable, degradable polymeric carrier for osteogenic cell populations. Part 1. Encapsulation of marrow stromal osteoblasts in surface crosslinked gelatin microparticles. *Biomaterials* **23**:4359–4371 (2002).
6. A. Gutowska, B. Jeong, and M. Jasionowski. Injectable gels for tissue engineering. *Anat. Rec.* **263**:342–349 (2001).
7. S. Wee and W. R. Gombotz. Protein release from alginate matrices. *Adv. Drug Deliv. Rev.* **31**:267–285 (1998).
8. C. K. Kuo and P. X. Ma. Ionically crosslinked alginate hydrogels as scaffolds for tissue engineering: part 1. Structure, gelation rate and mechanical properties. *Biomaterials* **22**:511–521 (2001).
9. B. J. Spargo, A. S. Rudolph, and F. M. Rollwagen. Recruitment of tissue resident cells to hydrogel composites: *in vivo* response to implant materials. *Biomaterials* **15**:853–858 (1994).
10. M. Otterlei, K. Ostgaard, G. Skjak-Braek, O. Smidsrod, P. Soon-Shiong, and T. Espevik. Induction of cytokine production from human monocytes stimulated with alginate. *J. Immunother.* **10**:286–291 (1991).
11. N. E. Simpson, C. L. Stabler, C. P. Simpson, A. Sambanis, and I. Constantinidis. The role of the CaCl2-guluronic acid interaction on alginate encapsulated betaTC3 cells. *Biomaterials* **25**:2603–2610 (2004).
12. J. A. Rowley, G. Madlambayan, and D. J. Mooney. Alginate hydrogels as synthetic extracellular matrix materials. *Biomaterials* **20**:45–53 (1999).
13. L. Meinel, O. Illi, J. Zapf, M. Malfanti, H. P. Merkle, and B. Gander. Stabilizing insulin-like growth factor-I in poly(D,L-lactide-co-glycolide) microspheres. *J. Control. Release* **70**(1–2): 193–202 (2001).
14. L. Meinel, E. Zoidis, J. Zapf, P. Hassa, M. O. Hottiger, J. A. Auer, R. Schneider, B. Gander, V. Luginbuehl, R. Bettschart-Wolfisberger, O. E. Illi, H. P. Merkle, and B. von Rechenberg. Localized insulin-like growth factor I delivery to enhance new bone formation. *Bone* **33**:660–672 (2003).
15. L. Meinel, O. E. Illi, J. Zapf, M. Malfanti, H. Peter Merkle, and B. Gander. Stabilizing insulin-like growth factor-I in poly(D, L-lactide-co-glycolide) microspheres. *J. Control. Release* **70**:193–202 (2001).
16. H. J. Kong, M. K. Smith, and D. J. Mooney. Designing alginate hydrogels to maintain viability of immobilized cells. *Biomaterials* **24**:4023–4029 (2003).
17. C. Y. M. Tung and P. J. Dynes. Relationship between viscoelastic properties and gelation in thermosetting systems. *J. Appl. Polym. Sci.* **27**:569–574 (1982).
18. K. Matsuzaka, X. F. Walboomers, J. E. de Ruijter, and J. A. Jansen. The effect of poly-L-lactic acid with parallel surface micro groove on osteoblast-like cells *in vitro*. *Biomaterials* **20**:1293–1301 (1999).
19. D. Byrom. *Biomaterials Novel Materials from Biological Sources*, Stockton Press, New York, 1991.
20. D. J. McQuillan, M. D. Richardson, and J. F. Bateman. Matrix deposition by a calcifying human osteogenic sarcoma cell line (SAOS-2). *Bone* **16**:415–426 (1995).
21. J. Clover and M. Gowen. Are MG-63 and HOS TE85 human osteosarcoma cell lines representative models of the osteoblastic phenotype? *Bone* **15**:585–591 (1994).
22. C. Farquharson, J. Milne, and N. Loveridge. Mitogenic action of insulin-like growth factor-I on human osteosarcoma MG-63 cells and rat osteoblasts maintained *in situ*: the role of glucose-6-phosphate dehydrogenase. *Bone Miner.* **22**:105–115 (1993).
23. K. Raile, R. Hille, S. Laue, A. Schulz, G. Pfeifer, F. Horn, and W. Kiess. Insulin-like growth factor I (IGF-I) stimulates proliferation but also increases caspase-3 activity, Annexin-V binding, and DNA-fragmentation in human MG63 osteosarcoma cells: co-activation of pro- and anti-apoptotic pathways by IGF-I. *Horm. Metab. Res.* **35**:786–793 (2003).
24. M. N. Pollak, C. Polychronakos, and M. Richard. Insulinlike growth factor I: a potent mitogen for human osteogenic sarcoma. *J. Natl. Cancer Inst.* **82**:301–305 (1990).
25. E. Murray, D. Provvedini, D. Curran, B. Catherwood, H. Sussman, and S. Manolagas. Characterization of a human osteoblastic osteosarcoma cell line (SAOS-2) with high bone alkaline phosphatase activity. *J. Bone Miner. Res.* **2**:231–238 (1987).
26. S. Takamizawa, Y. Maehata, K. Imai, H. Senoo, S. Sato, and R. Hata. Effects of ascorbic acid and ascorbic acid 2-phosphate, a long-acting vitamin C derivative, on the proliferation and differentiation of human osteoblast-like cells. *Cell Biol. Int.* **28**:255–265 (2004).
27. S. B. Rodan, Y. Imai, M. A. Thiede, G. Wesolowski, D. Thompson, Z. Bar-Shavit, S. Shull, K. Mann, and G. A. Rodan. Characterization of a human osteosarcoma cell line (Saos-2) with osteoblastic properties. *Cancer Res.* **47**: 4961–4966 (1987).

28. S. A. Goldstein, D. L. Wilson, D. A. Sonstegard, and L. S. Matthews. The mechanical properties of human tibial trabecular bone as a function of metaphyseal location. *J. Biomech.* **16**: 965–969 (1983).
29. H. K. Koerten and J. van der Meulen. Degradation of calcium phosphate ceramics. *J. Biomed. Mater. Res.* **44**:78–86 (1999).
30. E. Alsberg, H. J. Kong, Y. Hirano, M. K. Smith, A. Albeiruti, and D. J. Mooney. Regulating bone formation via controlled scaffold degradation. *J. Dent. Res*. **82**:903–908 (2003).
31. F. Gu, B. Amsden, and R. Neufeld. Sustained delivery of vascular endothelial growth factor with alginate beads. *J. Control. Release* **96**:463–472 (2004).
32. R. J. Laham, F. W. Sellke, E. R. Edelman, J. D. Pearlman, J. A. Ware, D. L. Brown, J. P. Gold, and M. Simons. Local perivascular delivery of basic fibroblast growth factor in patients undergoing coronary bypass surgery: results of a phase I randomized, double-blind, placebo-controlled trial. *Circulation* **100**:1865–1871 (1999).
33. M. L. Springer, G. Hortelano, D. M. Bouley, J. Wong, P. E. Kraft, and H. M. Blau. Induction of angiogenesis by implantation of encapsulated primary myoblasts expressing vascular endothelial growth factor. *J. Gene Med.* **2**:279–288 (2000).
34. M. L. Springer, T. K. Ip, and H. M. Blau. Angiogenesis monitored by perfusion with a space-filling microbead suspension. *Molec. Ther.* **1**:82–87 (2000).
35. M. C. Peters, B. C. Isenberg, J. A. Rowley, and D. J. Mooney. Release from alginate enhances the biological activity of vascular endothelial growth factor. *J. Biomater. Sci., Polym. Ed.* **9**:1267–1278 (1998).
36. Y. M. Elcin, V. Dixit, and G. Gitnick. Extensive *in vivo* angiogenesis following controlled release of human vascular endothelial cell growth factor: implications for tissue engineering and wound healing. *Artif. Organs* **25**:558–565 (2001).
37. M. E. Svoboda, J. J. van Wyk, D. G. Klapper, R. E. Fellows, F. E, Grissom, and R. J. Schlueter. Purification of somatomedin-C from human plasma: chemical and biological properties, partial sequence analysis, and relationship to other somatomedins. *Biochemistry* **19**:790–797 (1980).
38. J. Zapf, E. Schoenle, and E. R. Froesch. Insulin-like growth factors I and II: some biological actions and receptor binding characteristics of two purified constituents of nonsuppressible insulin-like activity of human serum. *Eur. J. Biochem.* **87**:285–296 (1978).
39. A. Haug. *Composition and Properties of Alginates*, Norwegian Institute of Technology, Trondheim, 1964.
40. D. Malamud and J. Drysdale. Isoelectric points of proteins: a table. *Anal. Biochem.* **86**:620–647 (1978).
41. D. S. Steinbrech, B. J. Mehrara, N. M. Rowe, M. E. Dudziak, P. B. Saadeh, G. K. Gittes, and M. T. Longaker. Gene expression of insulin-like growth factors I and II in rat membranous osteotomy healing. *Ann. Plast. Surg.* **42**:481–487 (1999).
42. E. Solheim. Growth factors in bone. *Int. Orthop.* **22**:410–416 (1998).
43. T. J. Cho, L. C. Gerstenfeld, and T. A. Einhorn. Differential temporal expression of members of the transforming growth factor beta superfamily during murine fracture healing. *J. Bone Miner. Res.* **17**:513–520 (2002).
44. S. Dedhar, M. D. Mitchell, and M. D. Pierschbacher. The osteoblast-like differentiated phenotype of a variant of MG-63 osteosarcoma cell line correlated with altered adhesive properties. *Connect. Tissue Res.* **20**:49–61 (1989).
45. P. A. Conget and J. J. Minguell. Phenotypical and functional properties of human bone marrow mesenchymal progenitor cells. *J. Cell. Physiol.* **181**:67–73 (1999).
46. J. S. Sun, Y. H. Tsuang, C. J. Liao, H. C. Liu, Y. S. Hang, and F. H. Lin. The effects of calcium phosphate particles on the growth of osteoblasts. *J. Biomed. Mater. Res.* **37**:324–334 (1997).